

Local orientation variations in YBCO films on technical substrates - a combined SEM and EBSD study

Patrick Pahlke, Max Sieger, Paul Chekhonin, Werner Skrotzki, Alexander Usoskin, Jan Strömer, Jens Hänisch, Ludwig Schultz, Ruben Hühne

Abstract—Scanning electron microscope imaging and electron backscatter diffraction are applied to 400 nm thick YBCO films grown on Ni-9at.%W and ABAD-YSZ tape. On the Ni-9at.%W tape, the orientation distribution varies strongly from grain to grain, which is attributed to the different orientation of the Ni-grains with regard to the surface normal. On ABAD-YSZ the structures causing the orientation variations are observed in micrometer scale only, which is attributed to the granularity of the template. In contrast to Ni-9at.%W, where no preferred misorientation axis is notable within single Ni-grains, the orientation distribution of YBCO on the ABAD-YSZ tape is primarily caused by lattice rotations about the sample normal.

Index Terms—coated conductors, EBSD, PLD, YBCO

I. INTRODUCTION

THE template used for the preparation of $\text{YBa}_2\text{Cu}_3\text{O}_{7-\delta}$ (YBCO) based coated conductors affects the superconducting properties in multiple ways. It is therefore essential to understand how the template influences the structural and crystalline quality of the YBCO film.

The major techniques to achieve a biaxially textured tape are rolling assisted biaxially textured substrates (RABiTS) and ion beam assisted deposition (IBAD) [1]. The RABiTS approach is based on a rolling and annealing treatment of a Ni-based alloy, which leads to a strong recrystallization texture with biaxially aligned grains. In highly alloyed Ni-9at.%W tapes, the Curie point is strongly suppressed compared to tapes with lower W content leading to a reduction of AC losses at low temperatures [2], while still showing a 96% fraction of cube texture ($< 10^\circ$ criterion) [3]. In contrast, the IBAD approach is applied to polycrystalline substrates. The textured layer is created by an assisting ion-beam during deposition, leading to a biaxial alignment of the deposited material. A special form of IBAD is alternating beam assisted deposition (ABAD) to preferentially orient Y_2O_3 -stabilized ZrO_2 (YSZ).

This work was supported by EUROTAPES, a collaborative project funded by the European Commission's Seven Framework Program (FP7 / 2007 - 2013) under Grant Agreement n.280432. (Corresponding author: P. Pahlke)

P. Pahlke, M. Sieger, and L. Schultz are with IFW Dresden, 01069 Dresden, Germany and also with Dresden University of Technology, 01062 Dresden, Germany (e-mail: p.pahlke@ifw-dresden.de)

P. Chekhonin and W. Skrotzki are with Dresden University of Technology, 01069 Dresden, Germany (e-mail: werner.skrotzki@tu-dresden.de)

A. Usoskin and J. Strömer are with Bruker HTS GmbH, 63755 Alzenau, Germany (e-mail: alexander.usoskin@bruker-hts.com)

J. Hänisch is with the Karlsruhe Institute of Technology, Germany (e-mail: jens.haenisch@kit.edu)

R. Hühne is with IFW Dresden, 01069 Dresden, Germany (e-mail: r.huehne@ifw-dresden.de).

Here the deposition and ion-beam zone are separated [4].

The goal of this paper is a qualitative comparison of the local structure and the orientation distribution of YBCO deposited on Ni-9at.%W and ABAD-YSZ tapes. The results presented are also valid for tapes with lower W content, as these show a similar local structure.

II. EXPERIMENTAL

A. Sample Preparation

YBCO was deposited on two kinds of technical tapes: a RABiTS Ni-9at.%W tape with a PLD- $\text{Y}_2\text{O}_3/\text{YSZ}/\text{CeO}_2$ buffer layer system and a stainless steel tape with a PLD- CeO_2 buffered ABAD-YSZ layer. The YBCO layer was deposited by pulsed laser deposition (PLD) from a stoichiometric target on both templates arranged side by side in order to guarantee best comparison. A KrF excimer laser ($\lambda = 248$ nm, Coherent LPXpro 305) was used to deposit 3000 pulses YBCO at a laser repetition rate of 10 Hz leading to a layer thickness of around 400 nm. During deposition an oxygen pressure of 0.4 mbar and a temperature of 810 °C were maintained. To achieve optimally doped YBCO a subsequent oxygenation under an oxygen partial pressure of 400 mbar at 770 °C completed the process.

B. Structural characterization

The samples were analyzed by taking secondary electron images with a JEOL JSM-6510 scanning electron microscope (SEM) at an acceleration voltage of 20 kV.

Electron backscatter diffraction (EBSD) investigations were performed using a GEMINI LEO 1530 SEM with a Nordlys EBSD detector and the HKL Channel 5 acquisition software. An acceleration voltage of 20 kV, a 2 x 2 binning of the EBSD detector screen and a long exposure time of at least 0.4 seconds per EBSD pattern (EBSP) were used to achieve high quality patterns.

The recorded EBSPs were first saved on the hard disk and indexed after the measurements. This procedure has several advantages. First, it conserves CPU resources so that the measurement can be performed faster, reducing contamination and possible errors due to beam or focus drift. Second, the EBSPs can be analyzed in a post-process with different sets of parameters to achieve a high indexing rate. Third, EBSPs can be manually indexed afterwards, which allows to check for wrongly indexed points in the mapping. To avoid beam drift, the setup including an active electron beam was prepared several hours prior to the EBSD measurement.

The EBSD mappings were created with the Oxford Instru-

ments HKL Channel 5 Software using the advanced fit option for smaller random errors. The extrapolation option down to level 6 and the wild spike extrapolation was applied.

The automatic indexing of the recorded EBSPs using the orthorhombic YBCO phase available in the HKL database was not satisfying, because it often led to wrong solutions. Therefore, a related tetragonal cuprate phase with a slightly higher c/a ratio was used instead. By manually indexing a set of EBSPs using the YBCO and the tetragonal phase it was found that the misorientation between different EBSPs is overrated by about 10% with respect to the real situation. Therefore, the misorientation values given in this paper are slightly higher than in reality. From orientation profiles on homogeneous grain areas, the random error of the orientation data was estimated to $< 0.2^\circ$, thus allowing a detailed misorientation analysis. This is in agreement with a previous publication [5], where an even smaller random error was measured using a comparable experimental EBSD setup and the same evaluation software.

III. RESULTS

A. SEM investigation

The kind of template apparently affects the growth of the YBCO thin film as already visible on the $50\ \mu\text{m}$ scale in SEM images (Fig. 1). YBCO grows very homogeneous on the ABAD tape and only a few pores are visible. On the Ni-9at.%W tape the situation is quite different. The legacy of the recrystallized grains of the Ni-9at.%W tape with a typical grain size of $20\ \mu\text{m}$ to $50\ \mu\text{m}$ can be clearly seen. Because the Ni9at.%W grains are misoriented against each other, the surface of each single Ni grain can be understood as a template with an individual crystallographic miscut towards the substrate normal. Depending on the miscut angle, the YBCO can grow smooth and dense (blue arrows in Fig. 1) or faceted and porous (red arrows in Fig. 1). The direction and width of the facets are varying from grain to grain. Measurements performed by atomic force microscopy revealed a terrace width of around $400\ \text{nm}$ and a step height of around $50\ \text{nm}$ for one selected grain. The corresponding inclination angle can be calculated to $\sim 7^\circ$, which is a reasonable value (see Fig. 3). This terrace morphology strongly reminds of YBCO grown on inclined substrate deposition (ISD) tapes (see [6], [7]). There, the inclination is constant over the whole tape width.

Regions with large pores (green arrow in Fig. 1 (b)) and segregations (white particles in Fig. 1 (b)) are also found. The density of segregations (most probably CuO_x particles) is quite different on each single grain. Some grains are totally free while others are full of such particles. It is assumed that the ability to form these segregations is strongly correlated to the individual miscut angle of the related substrate grain.

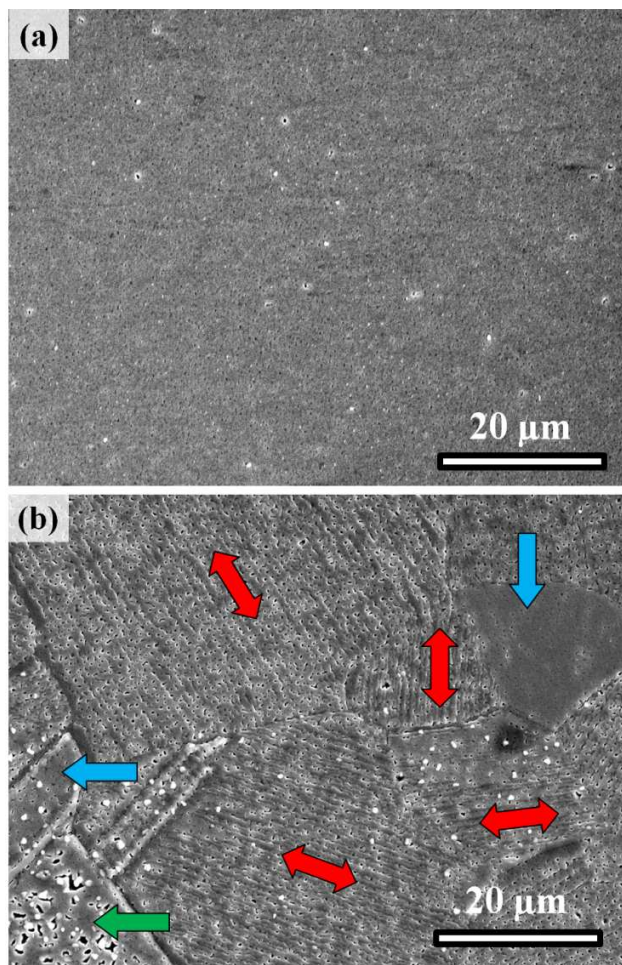


Fig. 1. SEM image of YBCO deposited on (a) ABAD-YSZ and (b) Ni-9at.%W tape. The blue arrows are pointing to flat grain surfaces whereas the green arrow points to a grain with large pores. The red arrows indicate the direction of terraces in the faceted grain surfaces.

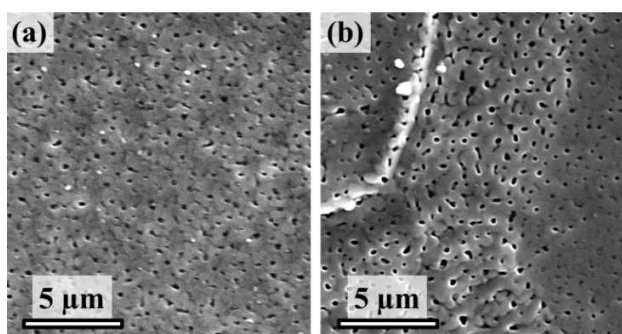


Fig. 2. Higher magnification SEM image of YBCO deposited on (a) ABAD-YSZ and (b) Ni-9at.%W tape.

At higher magnification (Fig. 2) the structure of merging YBCO islands (areas between pores, estimated upper grain size $0.3\ \mu\text{m} - 0.8\ \mu\text{m}$) is visible on both templates. The islands appear rather round on the ABAD tape, whereas they are more elongated on the Ni-9at.%W tape. Additionally, the surface roughness and the density as well as size of pores vary more strongly on the Ni-9at.%W tape.

B. EBSD investigation - mappings

In general, YBCO grows epitaxially on the provided templates except on highly misoriented areas such as recrystallization twins [8]. Therefore, the granular structure of the underlying Ni-9at.%W tape is still observable on the 100 μm -scale in the EBSD mappings (Fig. 3). The majority of grains are highly cube oriented with deviations from ideal of less than 12° , only a few areas ($< 5\%$) exhibit larger values (black points in Fig. 3). The substructure within a substrate grain means that the orientation of YBCO growing on a single grain of the template is not constant. This local orientation distribution is very different from grain to grain and may be the result of the lattice misfit accommodation as well as the adjustment to the local surface structure. The misorientation within a grain is clearly visible in EBSD mappings with a small step size (Fig. 4).

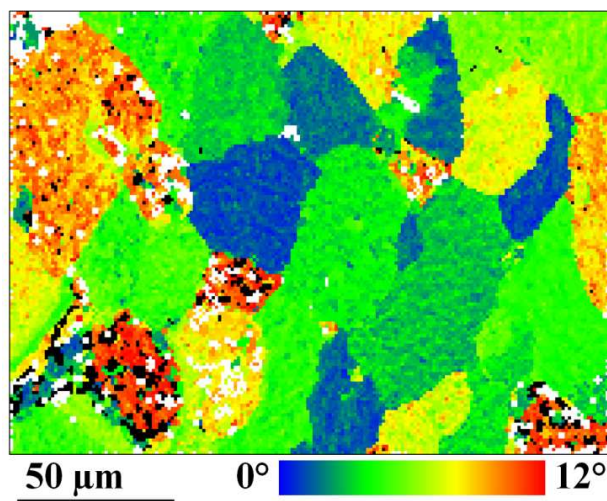


Fig. 3. EBSD mapping (step size 1 μm) of YBCO deposited on Ni-9at.%W tape showing the absolute misorientation from the ideal cube texture. White dots are non-indexed areas, at black dots the misorientation exceeds 12° .

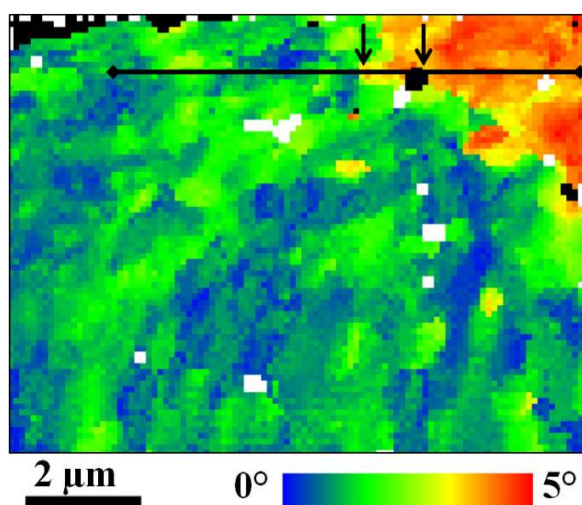


Fig. 4. EBSD mapping (step size 0.1 μm) of YBCO deposited on Ni-9at.%W tape showing the absolute misorientation from the ideal cube texture. White dots are non-indexed areas, at black dots the misorientation exceeds 5° . The black line indicates the position of the line scan and the arrows point to the location of grain boundaries.

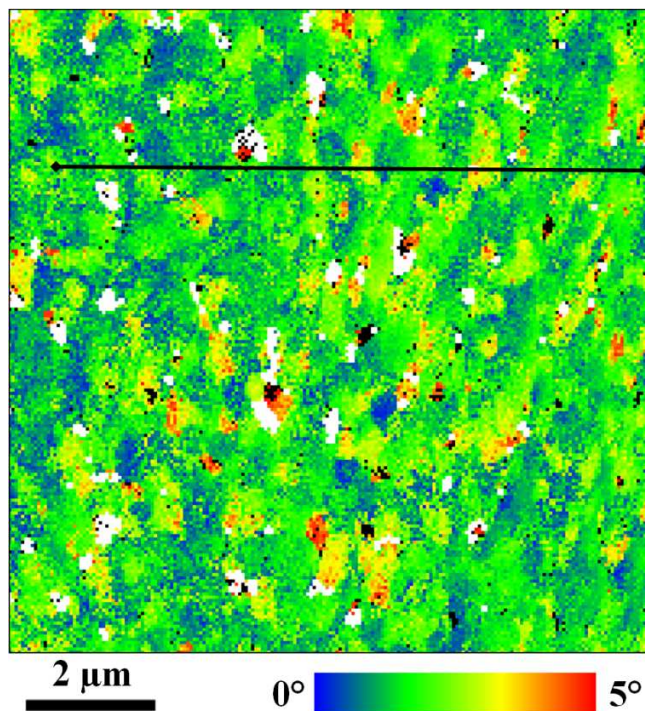


Fig. 5. EBSD mapping (step size 0.05 μm) of YBCO deposited on ABAD-YSZ tape showing the absolute misorientation from the ideal cube texture. White dots are non-indexed areas, at black dots the misorientation exceeds 5° . The black line indicates the position of the line scan.

The situation is different for the ABAD tape. This template is homogeneous and therefore granularity of the YBCO film is not observed on the 100 μm -scale. Granularity is first seen in EBSD mappings with a step size below 100 nm (Fig. 5). Only very few sites ($\sim 1\%$) of the YBCO film show a misorientation larger than 5° .

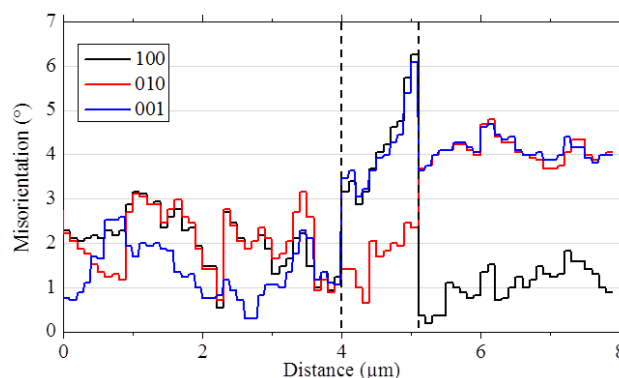


Fig. 6. EBSD line scan across an area of the EBSD mapping Fig. 4 of YBCO deposited on Ni-9at.%W tape (step size 0.1 μm). The three plotted lines show the angular deviation of the [100]-, [010]- and [001]-YBCO axis from the rolling, transverse and normal direction of the thin film, respectively. The location of the grain boundaries is indicated by dotted lines.

C. EBSD investigation - line scans

The EBSD mappings discussed in the previous section show the misorientation angle with respect to the ideal cube

orientation. This information alone is insufficient for determining the rotation axis. To analyze this, the angular deviation of the [100]-, [010]- and [001]-YBCO axis from the rolling, transverse and normal direction of the thin film, respectively, needs to be taken into account. Instead of showing additional mappings for each of the three rotation axis, line scans across these images have been done and combined in angular deviation-distance graphs (Fig. 6 and Fig. 7). The positions of the line scans are shown in the EBSD mappings in Fig. 4 and Fig. 5.

For the Ni-9at.%W tape, the line scan crosses two grain boundaries (arrows in Fig. 4 and dotted lines in Fig. 6). Along the chosen line scan an internal angular deviation (within one grain) with respect to all three sample axes can be observed. The curves for different sample axes are not always correlated, which means, that the lattice rotations do not have a preferred rotation axis. However, the internal angular deviations are limited to about 3° .

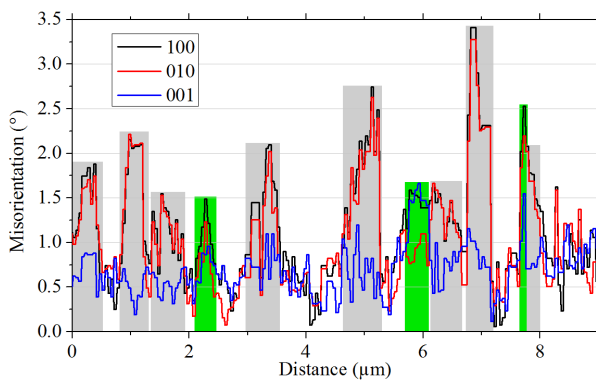


Fig. 7. EBSD line scan across an area of the EBSD mapping Fig. 5 of YBCO deposited on ABAD-YSZ tape (step size $0.05 \mu\text{m}$). The three plotted lines show the angular deviation of the [100]-, [010]- and [001]-YBCO axis from the rolling, transverse and normal direction of the thin film, respectively. Note the equal length scale, but the different misorientation scale compared to Fig. 6.

On the ABAD tape the normal direction of the thin film is found to be an invariant rotation axis (Fig. 7). There is almost no deviation of the [001] YBCO axis from the normal direction (few exceptions marked green in Fig. 7), while the angular deviation of the [100]- and [010]-YBCO axis from the rolling and transverse direction, respectively, strongly correlate and overlap in most parts (gray areas in Fig. 7). The angular deviation of the [001] YBCO axis from the normal direction is as low as 1° . The high grade of c -axis alignment is confirmed by global texture measurements with a peak full width at half maximum (FWHM) of $\sim 1.4^\circ$ for an ω -scan of the YBCO (005) peak. Corresponding measurements on the Ni-9at.%W tape yield a FWHM of $\sim 2.2^\circ$. The angular deviation of the [100]- and [010]-YBCO axis from the rolling and transverse direction shows typically values of 1° to 3° (Fig. 7). These values appear generally comparable to the internal misorientation distribution on grains of the Ni-9at.%W tape (Fig. 6).

IV. DISCUSSION

The origin of the internal misorientation of YBCO on Ni-9at.%W tapes may be due to different miscut angles of the underlying Ni-grain: On grains with almost no miscut, YBCO finds nearly single crystalline growth conditions and therefore exhibits a sharp texture, whereas on a strongly tilted grain, YBCO grows in facets and with formation of pores leading to local rotations of the YBCO unit cell and a broader local orientation distribution.

The YSZ layer of the ABAD tape is textured due to growth selection during the IBAD step [9]. The evolving YSZ grains show columnar growth and are slightly misoriented against each other. From TEM investigations on related samples the diameter of the columnar grains is estimated to be between 200 nm to 300 nm. In previous studies also some kind of growth selection was observed in the YBCO layer itself, leading to an increased grain size and sharper texture with increasing film thickness [10]. Therefore, those areas where the sample normal direction appears to be the sole major rotation axis (marked grey in Fig. 7) may be attributed to single or a few merged YBCO grains. This idea is supported by the SEM observation described in section III. A.: the size of single or a few coalescent grains matches with the structural dimensions in the EBSD mappings (Fig. 5) and the line scans (Fig. 7).

V. CONCLUSION

The SEM and EBSD investigations reveal a microstructure of YBCO which is highly influenced by the template material. On Ni-9at.%W tape the YBCO grows on Ni-grains with different miscut angles, leading to a diverse microstructure, ranging from dense and flat to porous and faceted areas. This may explain the large variations of the internal misorientation amplitudes from all sample axes. Although locally a correlation between the angular deviations from two sample axes is observed, there does not exist a preferred misorientation axis.

YBCO is growing homogeneously on ABAD templates and structural features are first observed on the micrometer scale. The major part of the misorientation from the ideal cube orientation is caused by a rotation of the YBCO lattice around the sample normal. The length scale of the misoriented areas matches very well with the grain size of the ABAD template.

ACKNOWLEDGMENT

We thank David Geißler for inspiring discussion.

REFERENCES

- [1] X. Obradors and T. Puig, "Coated conductors for power applications: materials challenges", *Supercond. Sci. Technol.*, vol. 27, no. 4, 044003, Apr. 2014.
- [2] U. Gaitzsch et al., "Highly alloyed Ni-W substrates for low AC loss applications", *Supercond. Sci. Technol.*, vol. 26, no. 8, 085024, Aug. 2013.
- [3] J. Eickemeyer et al., "Textured Ni-9.0% W substrate tapes for YBCO-coated conductors", *Supercond. Sci. Technol.*, vol. 23, no. 8, 085012, 2010.
- [4] A. Usoskin et al., "Processing of long-length YBCO coated conductors based on stainless steel tapes", *IEEE Trans. Appl. Supercond.*, vol. 17, no. 2, pp. 3235-3238, Jun. 2007.

- [5] P. Chekhonin, J. Engelmann, C.-G. Oertel, B. Holzapfel and W. Skrotzki, "Relative angular precision in electron backscatter diffraction: A comparison between cross correlation and Hough transform based analysis", *Cryst. Res. Technol.*, vol. 49, no. 6, pp. 435-439, Jun. 2014.
- [6] K. K. Uprety, B. Ma, R. E. Koritala, B. L. Fisher, S. E. Dorris and U. Balachandran, "Growth and properties of YBCO-coated conductors on biaxially textured MgO films prepared by inclined substrate deposition", *Supercond. Sci. Technol.*, vol. 18, no. 3, pp. 294-298, Mar. 2005.
- [7] B. Ma et al., "Growth and properties of YBCO-coated conductors fabricated by inclined-substrate deposition", *IEEE Trans. Appl. Supercond.*, vol. 15, no. 2, pp. 2970-2973, Jun. 2005.
- [8] R. Hühne et al., "Application of textured highly alloyed Ni-W tapes for preparing coated conductor architectures", *Supercond. Sci. Technol.*, vol. 23, no. 3, 034015, Mar. 2010.
- [9] J. Dzick, J. Hoffmann, S. Sievers, L. O. Kautschor and H. C. Freyhardt, "Ion-beam-assisted texturing of YSZ layers", *Physica C.*, vol. 372-376, no. 2, pp. 723-728, Aug. 2002.
- [10] P. Pahlke et al., "Thick High J_c YBCO Films on ABAD-YSZ Templates", *IEEE Trans. Appl. Supercond.*, vol. 25, no. 3, 6603804, Jun. 2015.